$$(\lambda_0 + \lambda_1)\eta = T_c\eta \quad (1)$$

yields T_c(pristine) = $\lambda_0 + \lambda_1$.

For stage-1 $IBi_2Sr_2CaCu_2O_x$, the model is the same but with λ_1 replaced by λ_1' because the next nearest plane coupling is assumed to be grossly affected by the intercalation. The predicted stage-1 T_c is then $\lambda_0 + \lambda_1'$.

For stage-2 $IBi_4Sr_4Ca_2Cu_4O_x$, the CuO_2 planes are no longer equivalent; there are planes (a) coupled by λ_0 and λ_1 and planes (b) coupled by λ_0 and λ_1'. The eigenvalue equation for T_c is then

$$T_c\begin{pmatrix}\eta_a\\ \eta_b\end{pmatrix} = \begin{bmatrix}\lambda_1 & \lambda_0\\ \lambda_0 & \lambda_1'\end{bmatrix}\begin{pmatrix}\eta_a\\ \eta_b\end{pmatrix} \quad (2)$$

If we assume that intercalation completely destroys the next nearest plane coupling, then $\lambda_1' \to 0$, and the measured T_c(stage-1) yields λ_0 = 80 K. With T_c(stage-2) = 85 K, λ_0 = 80 K, and λ_1' = 0 K, we find λ_1 = 9.7 K. This is consistent with the results for the pristine material, where T_c is typically 90 K [= ($\lambda_0 + \lambda_1$)].

It is possible to use the above analysis to predict the T_c's for higher stage compounds. If λ_0 = 80 K, λ_1 = 10 K, and λ_1' = 0 K, the predicted T_c's for stages 3, 4, 5, and 6 are 87, 88, 89, and 89 K, respectively. Although we have demonstrated that stage-3 and stage-4 structures exist for iodine-intercalated $Bi_2Sr_2CaCu_2O_x$, we have not been able to reliably determine the T_c's for these minority phases.

A second approach incorporates interplane interactions into a Bardeen-Cooper-Schrieffer (BCS)–like framework. Such a model has been advanced by Ihm and Yu (7), although they neglected interblock coupling. Because our experiments indicate that this coupling cannot be neglected, we incorporate such a coupling into a phenomenological model (which is essentially an extension of the original work of Ihm and Yu).

Solving the BCS-like gap equations, assuming a constant density of states per CuO_2 plane (even after intercalation), one obtains

$$F(\text{pristine}) = \left(\frac{1}{\lambda_a + \lambda_{er} + \lambda_n}\right) \quad (3)$$

$$F(\text{stage-1}) = \left(\frac{1}{\lambda_a + \lambda_{er}}\right) \quad (4)$$

$$F(\text{stage-2}) \approx \left(\frac{1}{\lambda_a + \lambda_{er} + \frac{\lambda_n}{2}}\right) \quad (5)$$

$$F(\text{Bi-2223}) = \left(\frac{1}{\lambda_a + \sqrt{2}\lambda_{er} + \lambda_n}\right) \quad (6)$$

where $F(\Delta_\epsilon) = \int_0^{\hbar\omega} \tanh[(\epsilon^2 + \Delta_\epsilon^2)^{1/2}/2kT]/(\epsilon^2 + \Delta_\epsilon^2)^{1/2} d\epsilon$ is the gap function ($\hbar$ is Planck's constant divided by 2π, ω is frequency, ϵ is energy, k is Bolzmann's constant; $\lambda_a(\lambda_{er})$ is $N(\epsilon_f)V_a$ [$N(\epsilon_f)V_{er}$], the intraplane and nearest CuO_2 plane couplings (7); and λ_n is $N(\epsilon_f)V_n$, the next block coupling [$N(\epsilon_f)$ is the density of states at the Fermi level, and V is the strength of the interaction].

In this model, F determines T_c through $kT_c \cong 1.14\ \hbar\omega \exp(-F)$. If we fit the coupling parameters λ_a, λ_{er}, and λ_n for $\hbar\omega$ = 0.1 eV to the experimentally determined T_c's of pristine $Bi_2Sr_2Ca_2Cu_3O_x$ (Bi-2223) (T_c = 110 K) and the pristine and stage-1 $IBi_2Sr_2CaCu_2O_x$ compounds, we obtain λ_a = 0.2840, λ_{er} = 0.0725, and λ_n = 0.0156. Although λ_n is small (~5% of λ_a), it is over 20% of the size of λ_{er} and not negligible. With these parameters, this model predicts the stage-2 T_c to be 84.9 K, in excellent agreement with the experimentally determined T_c = 85 K. Hence, with interblock coupling included, a BCS-like model accounts well for the intercalation-induced shift in T_c for the stage-2 material. The model can also be extended to predict the T_c's of higher stage compounds, although the dependence of F on the coupling is much more complex than for lower stages.

In conclusion, we have shown that high-stage iodine intercalation of $Bi_2Sr_2CaCu_2O_x$ is possible. The shifts in T_c of the intercalated materials demonstrate that interblock coupling is an important ingredient in describing high-T_c copper oxides. In $Bi_2Sr_2CaCu_2O_x$, coupling between each pair of adjacent CuO_2-containing blocks contributes ~5 K to T_c.

REFERENCES AND NOTES

1. X.-D. Xiang *et al.*, *Nature* **348**, 145 (1990); X.-D. Xiang *et al.*, *Phys. Rev. B* **43**, 11496 (1991).
2. P. Levy, *Intercalated Layered Materials* (Reidel, Dordrecht, 1979).
3. X.-D. Xiang *et al.*, unpublished data.
4. D. H. Lowndes, D. P. Norton, J. D. Budai, *Phys. Rev. Lett.* **65**, 1160 (1990).
5. J.-M. Triscone, M. G. Karkut, L. Antognalla, A. Brunner, O. Fisher, *ibid.* **63**, 1016 (1989).
6. J. M. Wheatley, T. C. Hsu, P. W. Anderson, *Nature* **333**, 121 (1988).
7. J. Ihm and B. D. Yu, *Phys. Rev. B* **39**, 4760 (1989).

8. This work was supported by the director, Office of Energy Research, Office of Basic Energy Sciences, Materials Sciences Division of the U.S. Department of Energy under contract DE-AC03-76SF00098. J.L.C., T.W.B., and M.L.C. were also supported by National Science Foundation grant DMR88-18404. J.L.C. acknowledges support from an AT&T Ph.D. fellowship. M.L.C. acknowledges support from the J.S. Guggenheim Foundation.

10 September 1991; accepted 4 October 1991

Phase Transformations in Carbon Fullerenes at High Shock Pressures

C. S. YOO AND W. J. NELLIS

C_{60} powders were shock-compressed quasi-isentropically and quenched from pressures in the range 10 to 110 GPa (0.1 to 1.1 Mbar). Recovered specimens were analyzed by Raman spectroscopy and optical microscopy. C_{60} fullerenes are stable into the 13- to 17-GPa pressure range. The onset of a fast (~0.5 μs) reconstructive transformation to graphite occurs near 17 GPa. The graphite recovered from 27 GPa and about 600°C is relatively well ordered with crystal planar domain size of about 100 Å. Above 50 GPa a continuous transformation to an amorphous state is observed in recovered specimens. The fast transformation to graphite is proposed to occur by π-electron rehybridization which initiates breakup of the ball structure and formation of the graphite structure at high density.

THE FULLERENE MOLECULES (C_{60}) have a high-symmetry truncated icosahedral structure (*1*), which is very stable, despite the hollow cage with large strains in π-bonds and inherent structural "defects," the five-membered rings (*2*). The pseudospherical structure of C_{60} with diameter d_a = 7.1 Å is stable to a pressure of at least 20 GPa (200 kbar) at ambient temperature (*3*) and theoretically to 1800 K at ambient pressure (*4*). Introducing metal atoms between C_{60} balls induces little structural distortion (*5*). The exceptional stability of C_{60} is a central issue for developing new materials such as lubricants, ultrastrong fibers, hard materials, and high-temperature superconductors (*6*). For this reason it is important to determine the stability range of fullerenes at high pressures and temperatures.

C_{60} crystals, fullerites, order in a face-centered cubic (fcc) phase (*7*) with an extraordinarily weak van der Waals interaction between molecules, which causes a large compressibility at low static pressures (*3*).

Physics Department, H Division and Institute of Geophysics and Planetary Physics, Lawrence Livermore National Laboratory, University of California, Livermore, CA 94550.

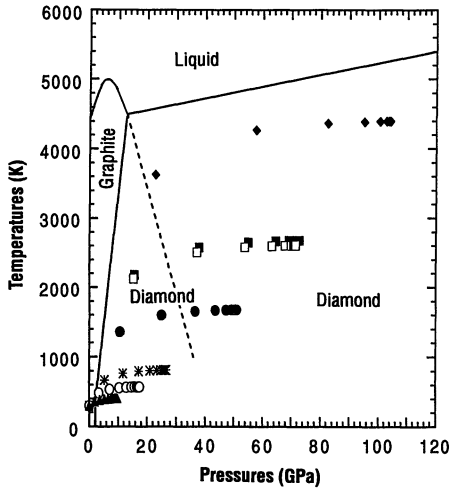

Fig. 1. The (P, T) paths of the multiple-shock experiments of C_{60} overlaid on the phase diagram of carbon. Each set of symbols represents the sequence of (P, T) points calculated for each multiple-shock experiment. The maximum pressure of each sequence is the pressure assigned to that specimen. The solid lines represent equilibrium phase boundaries and the dashed line represents the kinetic line for the direct graphite to diamond conversion. The phase boundary between diamond and liquid carbon is obtained from the theoretical calculation by van Thiel and Ree (*17*).

The fcc phase is relatively soft with a low-pressure bulk modulus of B_o = 18.1 GPa, which increases rapidly with a pressure coefficient of dB/dP = 5.7 (*3*). Although the fcc structure is stable to at least 20 GPa under hydrostatic pressure, it transforms to a lower symmetry structure at 16 to 20 GPa under nonhydrostatic conditions (*3*). Neither the crystal structure nor the molecular structure of C_{60} in the high-pressure phase has been reported.

Because of the unusual open structure of fullerenes, the nature of phase transitions in fullerites is of great interest over a wide range of pressures and temperatures. New high-pressure carbon phases have recently been observed experimentally or predicted theoretically, including n-diamond (*8*), transparent pressurized graphite (*9*), and BC-8 carbon (*10*). Fullerites might transform to as yet undiscovered phases. Fast shock-induced phase transformations provide information on the kinetics and possibly on the mechanisms of transformations. Typically, fast martensitic transitions are observed under shock compression, rather than slow reconstructive ones (*11*). In this report we present results on the range of molecular stability and phase transformations in fullerene powders, shock-compressed and quenched from pressures in the range of 10 to 110 GPa. Shock pressures in fullerenes are expected to be quasi-hydrostatic within the stability field of fullerenes because of the weak van der Waals interactions.

Bulk samples 10 mm in diameter and 100 to 150 μm thick were prepared by tapping C_{60} powders (*12*) to a density of 1.2 to 1.3 g cm^{-3}, approximately 75% of bulk crystal density of 1.65 g cm^{-3} (*7*). Thin specimens are used for rapid quenching of high-pressure phases. The powders are contained in a Cu sample capsule; the capsule is embedded in a steel recovery fixture (*13*). A planar shock wave is generated by accelerating a Cu impactor to velocities in the range of 1 to 3.5 km s^{-1} with a two-stage light-gas gun and impacting it onto a Cu capsule. The method is similar to shock-recovery experiments described elsewhere (*14*). The shocked samples were analyzed by Raman microprobe spectroscopy and optical microscopy.

Maximum pressure and temperature in a sample are achieved in about 50 ns by shock-wave reverberation between the Cu walls of the capsule. This loading is quasi-isentropic and produces much lower bulk temperatures than a single shock to the same pressure. Peak pressure is obtained to within 1% by measurement of impact velocity and the known equation of state of Cu. The sample remains at peak pressure for approximately 500 ns until the pressure release wave from the back of the impactor quenches the pressure and temperature isentropically. Residual temperature is quenched in the 100-μm thin sample by thermal diffusion into the Cu capsule. The pressure-temperature (P-T) history of the sample is obtained by shock-wave propagation calculations (*15*) that make use of equations of state for C_{60} and Cu. The equation of state for C_{60} is approximated with that of vitreous carbon powders (*16*). Temperatures are calculated with a Gruneisen thermal equation of state with γ = 0.35 (*17*) and an Einstein heat capacity model with θ_E = 1280 K (*18*). Peak sample temperatures are estimated to be about 550°C and 2200°C at peak pressures of 27 GPa and 70 GPa, respectively. The sequences of P-T states of the samples are shown in Fig. 1 along with the equilibrium phase diagram of carbon. In these multiple-shock experiments the temperature increases to ~80% of the peak on the first pressure step, which is approximately 20% of the peak pressure.

Raman spectroscopy is useful to identify and characterize various forms of carbon (*19*). Raman spectra of unshocked and shocked C_{60} powders are shown in Fig. 2. The C_{60} spectrum at ambient pressure is similar to the reported one (*19*), except for the higher intensity of the 1565 cm^{-1} band caused by the higher concentration of C_{70}. The Raman spectrum of the samples recovered at 10 GPa and at 13 GPa (not shown) is nearly unchanged from that at ambient conditions. The 17-GPa spectrum clearly indicates mixed phases of C_{60} and graphite. The C_{60} to graphite transition is nearly completed at 27 GPa. At higher pressures mixtures of graphite and disordered carbon are recovered. As pressure and temperature increase, the relative intensity of the 2710 cm^{-1} band decreases, indicating increasing disorder in the graphite.

Graphite particles are easily recognized under an optical microscope by their shiny metallic luster. Graphite crystallites are ubiquitous in the samples recovered from between 17 and 70 GPa. The product recovered from 27 GPa is nearly pure graphite, consistent with the Raman spectra. At higher pressures, the content of disordered carbon in the mixture increases. Only a highly disordered carbon phase is observed in the sample recovered from 110 GPa. The nature of the disorder is not yet known. However, it is assumed to be caused by a decrease of crystallite size and, thereby, to an increase of

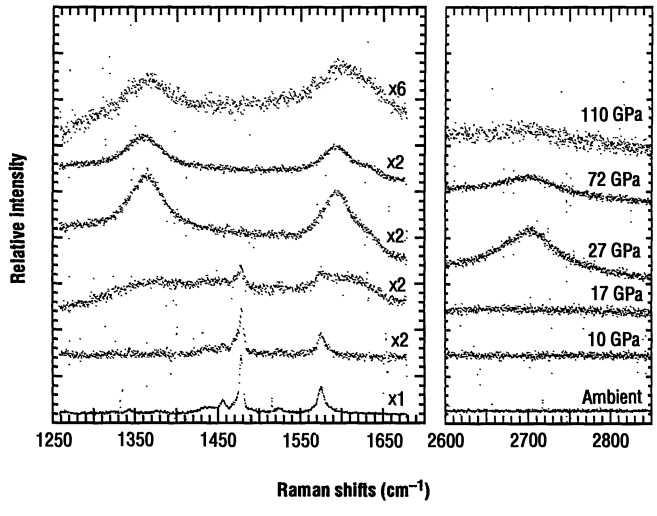

Fig. 2. Raman spectra of C_{60} and its shock recovered reaction products, showing transitions of C_{60} to graphite and to disordered carbon. The spectra are obtained at ambient pressure. The (P, T) paths of the experiments are shown in Fig. 1. The peak pressures are denoted in the figure. The ×1, ×2, and ×6 notations indicate the scaling factors of the spectra. The spectrum for 13 GPa (not shown) is similar to the 10-GPa spectrum.

sp^3 and sp bonding characters.

The 27-GPa Raman spectrum is characteristic of graphite which is relatively well ordered, especially for shock-synthesized material. The crystal planar domain size, L_a, is estimated to be about 100 Å, based on the relative intensities of the 1355, 1580, and 2710 cm^{-1} bands (*19*). This dimension corresponds to a graphitic sheet of 5 to 10 planar-reconstructed C_{60} molecules. The peak mean bulk temperature 600°C is substantially lower than typical graphite annealing temperatures of 2000° to 3000°C (*20*). Thus, the graphite is formed primarily by high pressure. However, strong heterogeneous shock-heating near pores may assist the graphite formation. The temperatures during or after the unloading processes are too low for forming ordered graphite. Increasing disorder in the graphite products, as pressure and temperature increase, is in marked contrast to conventional thermal annealing effects on graphite (*20*).

The synthesis of graphite near 17 GPa is consistent with the static pressure results. The C_{60} ball is extremely incompressible and its molecular structure essentially remains unchanged at moderately high pressures. However, the center to center distance between nearest neighbor C_{60} molecules collapses from 10.0 Å at ambient pressure to 7.82 Å at 17 GPa (*3*), which is comparable to the C_{60} diameter 7.1 Å (*1*). Interfullerene C–C distances at 17 GPa are, then, expected to be close to the C=C bond length in C_{60} and in graphite (*21*). Under these circumstances graphite can be formed through π-electron rehybridization (a fast process) without involving a great deal of atomic rearrangement (a slow diffusive process). That is, when the distance between C atoms on adjacent fullerenes approaches the C–C separation within a fullerene, bonding arrangements probably change from intrafullerene to interfullerene in such a way as to collapse balls into planar graphite. Fast reorientation of electronic bonds is, thus, expected to enable this reconstructive phase transformation on a submicrosecond time scale.

As shown in Fig. 1, the *P-T* paths of C_{60} shocked below 30 GPa remain in a region where the graphite phase is metastable. At higher shock pressures the sample is driven above the graphite-diamond kinetic line, where graphite transforms directly to diamond on a fast (microsecond) time scale (*22*). However, recovery of diamond depends strongly on thermal path, nucleation and growth kinetics, and thermal quench rates (*22*). Thus, diamond probably formed during compression in the 100-GPa range at temperatures above 3000 K, but reverted to amorphous carbon during pressure release because of an insufficient thermal quench rate.

REFERENCES AND NOTES

1. H. W. Kroto, J. R. Heath, S. C. O'Brien, R. F. Curl, R. E. Smalley, *Nature* **318**, 162 (1985); W. Krätschmer, L. D. Lamb, K. Fostiropoulos, D. R. Huffmann, *ibid.* **347**, 354 (1990).
2. H. Kroto, *Science* **242**, 1139 (1988); T. G. Schnalz, W. A. Seitz, D. J. Klein, G. E. Hite, *J. Am. Chem. Soc.* **110**, 1113 (1988).
3. S. J. Duclos, K. Brister, R. C. Haddon, A. R. Kortan, F. A. Thiel, *Nature* **351**, 380 (1991).
4. Q.-Z. Zhang, J.-Y. Yi, J. Bernholc, *Phys. Rev. Lett.* **66**, 2633 (1991).
5. K.-A. Wang *et al.*, *Phys. Rev. B*, in press.
6. E. Edelson, *Popular Science* **239**, 52 (August 1991); A. F. Hebard *et al.*, *Nature* **350**, 600 (1991); M. S. Dresselhaus and G. Dresselhaus, a private communication.
7. R. M. Fleming *et al.*, *Bull. Am. Phys. Soc.* **36**, 352 (1991).
8. H. Hirai and K. I. Kondo, *Science* **253**, 772 (1991).
9. W. Utsumi and T. Yagi, *ibid.* **252**, 1542 (1991).
10. C. Maihiot and A. K. McMahan, in preparation.
11. D. J. Erskine and W. J. Nellis, *Nature* **349**, 317 (1991); P. S. DeCarli and J. C. Jamieson, *Science* **133**, 1821 (1961).
12. The C_{60} powder was obtained from Research Co. (Golden, CO). It contains approximately 85% of C_{60} and 15% of C_{70} based on mass spectrographic analysis. The presence of 15% of C_{70} is expected to have a weak effect on the results because of the disordered fluid-like nature of powder specimens.
13. For the experiments at 70 and 110 GPa the C_{60} powder is sandwiched between millimeter-thick Cu plates. This sample assembly is then loaded in a stainless steel recovery capsule and a maraging steel fixture.
14. J. J. Neumeier *et al.*, *High Pressure Res.* **1**, 267 (1989).
15. A one-dimensional Lagrangian wave propagation program POT (Projectile On Target) is used in the calculation. This program was originally developed by G. E. Duvall.
16. W. H. Gust, *Phys. Rev.* **B22**, 4744 (1980).
17. M. van Thiel and F. H. Ree, *Int. J. Thermophys.* **10**, 227 (1989).
18. M. van Thiel, F. H. Ree, R. Grover, in *Shock Waves in Condensed Matter*, S. C. Schmidt and N. C. Holmes, Eds. (Elsevier, New York, 1988), pp. 81–84.
19. D. S. Knight and W. B. White, *J. Mat. Res.* **4**, 385 (1989); R. J. Nemanich and S. A. Solin, *Phys. Rev.* **B20**, 392 (1979); D. S. Bethune *et al.*, *Chem. Phys. Lett.* **179**, 181 (1991); also see K. A. Wang *et al.* (*5*).
20. Graphitization of carbon typically occurs by an annealing process at high temperatures of 2000° to 3000°C, and the better ordered graphite is formed at the higher annealing temperatures. The 27-GPa Raman spectrum in Fig. 2 is similar to that of graphite annealed at 2200°C or above, reported in the references: R. Vidano and D. B. Fischbach, *J. Am. Ceramic Soc.* **61**, 13 (1978); P. Lespade, A. Marchand, M. Couzi, F. Cruege, *Carbon* **22**, 375 (1984); Y. Hishiyama, M. Inagaki, S. Kimura, S. Yamada, *ibid.* **12**, 249 (1974).
21. The bond length changes in the sp^2 type bonds are typically less than a few percent at the pressure of 20 GPa. It may well be applied to a case of C_{60}. Assuming 2% reduction in the C=C bond length of C_{60}, the ball diameter is estimated to be 6.35 Å at 17 GPa. The interatomic C–C distances are then 1.51 Å, which is similar to the C=C bond lengths in C_{60} (two bond lengths in the C_{60} cluster are 1.46 Å and 1.40 Å) and in graphite (the C=C length in the plane is 1.42 Å). Furthermore, it is expected that 2% reduction in the C=C bonds in C_{60} at 17 GPa may represent an upper limit.
22. F. P. Bundy, *J. Geophys. Res.* **85**, 6930 (1980); A. V. Kurdyumov, N. F. Ostrovskaya, A. N. Pilyankevich, *Sov. Powder Metal. Met. Ceram.* **27**, 32 (1988); A. M. Staver, N. V. Gubareva, A. I. Lyamkin, E. A. Petrov, *Sov. Combustion Explosion Shock Waves* **20**, 567 (1980); also see (*11*).

23. We are pleased to acknowledge the contributions of N. Hinsey and W. Brocious for technical assistance and gun operations. We thank H. Cynn at UCLA for numerous discussions about C_{60} and N. C. Holmes, M. van Thiel, and F. H. Ree at LLNL for discussions about thermal properties of carbon. This work was performed under the auspices of the U.S. Department of Energy by Lawrence Livermore National Laboratory under contract number W-7405-ENG-48.

17 September 1991; accepted 28 October 1991

Symbiont Recognition and Subsequent Morphogenesis as Early Events in an Animal-Bacterial Mutualism

MARGARET J. MCFALL-NGAI AND EDWARD G. RUBY

Bacterial colonization of the developing light organ of the squid *Euprymna scolopes* is shown to be highly specific, with the establishment of a successful association resulting only when the juvenile host is exposed to seawater containing one of a subset of *Vibrio fischeri* strains. Before a symbiotic infection the organ has elaborate epithelial structures covered with cilia and microvilli that are involved in the transfer of bacteria to the incipient symbiotic tissue. These structures regressed within days following infection; however, they were retained in uninfected animals, suggesting that the initiation of symbiosis influences, and is perhaps a prerequisite for, the normal developmental program of the juvenile host.

BENEFICIAL ASSOCIATIONS WITH SPECIFIC bacterial symbionts characterize many, if not all, animal species. Yet the mechanisms that determine recognition and specificity, or that control subsequent morphogenesis, in developing animal-bacterial mutualisms have remained remarkably undescribed. The light organ symbiosis between the squid *E. scolopes* and its monospecific culture of the luminous bacterium *V. fischeri* exhibits experimental advantages not found in other commonly studied animal-bacterial mutualisms. Specifically, the host

Department of Biological Sciences, University of Southern California, Los Angeles, California 90089-0371.